

# Integrated active mixing and biosensing using surface acoustic waves (SAW) and surface plasmon resonance (SPR) on a common substrate

Alan Renaudin, Vincent Chabot, Etienne Grondin, Vincent Aimez and Paul G. Charette\*

Received 17th June 2009, Accepted 1st October 2009

First published as an Advance Article on the web 3rd November 2009

DOI: 10.1039/b911953a

This article presents a device incorporating surface plasmon resonance (SPR) sensing and surface acoustic wave (SAW) actuation integrated onto a common LiNbO<sub>3</sub> piezoelectric substrate. The device uses Rayleigh-type SAW to provide active microfluidic mixing in the fluid above the SPR sensor. Validation experiments show that SAW-induced microfluidic mixing results in accelerated binding kinetics of an avidin-biotin assay. Results also show that, though SAW action causes a parasitic SPR response due to heat injection into the fluid, a relatively brief relaxation time following the SAW pulses allows the effect to dissipate, without affecting the overall assay response. Since both SPR sensors and SAW transducers can be fabricated simultaneously using low-cost microfabrication methods on a single substrate, the proposed design is well-suited to lab-on-chip applications.

## Introduction

In recent years, point-of-care applications and high-throughput screening in the health care and pharmaceutical industries have led to a rapid development of affinity biosensors for the detection and analysis of biomolecular interactions.<sup>1</sup> Surface plasmon resonance (SPR) sensing is widely used for these applications due to several attractive features: it is label-free (*i.e.* no fluorescent tagging is required), real-time (allowing reaction kinetics to be measured), can be implemented in parallel (allowing high-throughput screening and the use of multiple targets), and can provide quantitative measurements.<sup>2</sup> Though several SPR systems are commercially available and have large established user bases, considerable research and development efforts continue both in universities and the private sector because cutting-edge medical, pharmaceutical, and environmental applications demand higher performance than current systems can deliver.<sup>3</sup>

In surface-based biosensing systems such as SPR, two particularly difficult challenges are:

(1) How to overcome sensitivity limitations due to non-specific adsorption<sup>4</sup> (here we use the term “sensitivity” in the most general sense, that is, the overall signal-to-noise ratio of the system resulting both from the specificity of the assay and the physical sensitivity of the transducer to all binding events). Non-specific adsorption is the weak binding of molecules other than the target analyte to the sensing surface, such as *via* long-range coulombic interactions. At best, this causes false positive readings and/or errors in quantitative estimates of analyte concentration. At worst, the nonspecifically adsorbed molecules can completely obscure the surface-bound ligands, inhibiting any contact with the target analyte.

(2) How to perform efficient mixing at the microfluidic level for homogeneous and timely analysis. To minimize the quantity of

expensive reagents, modern biosensing systems use microfluidics, where micro- or nano-litre sized fluid volumes are pumped through small channels having cross-section dimensions in the tens to hundreds of microns. Because the fluid flow at such small scales is laminar, the efficient mixing of reagents is a challenge in microfluidics. Under diffusion-limited conditions, incubation over several hours is often required to complete common surface biochemistry assays.<sup>5</sup>

The objective of the work presented here is to provide a single solution to the two challenges described above by integrating SPR sensing and surface acoustic wave (SAW) actuation on a common substrate. As explained in detail below, SAW can induce accelerated microfluidic mixing by acoustic streaming. In addition, SAW action has been shown to reduce and/or remove parasitic molecules nonspecifically bound to the surface (desorption), thereby increasing the measurement signal-to-noise ratio.

Microfluidics with SAW and SPR technologies are first briefly reviewed to demonstrate the relevance of the proposed system. A full description of our design combining SAW and SPR on a common substrate is then detailed and validation experiments are described.

## Shear-vertical (Rayleigh) surface acoustic waves (SV-SAW)

SAW are oscillations which propagate on the surface of a material. They can be generated using interdigitated transducers (IDT), fabricated using thin-film metal deposition on a piezoelectric substrate.<sup>6</sup> Typical systems use either a piezoelectric substrate or a non-piezoelectric substrate coated with a piezoelectric film.<sup>7</sup> The nature and directional cut of the piezoelectric material determine what type of SAW are generated, either “shear-horizontal” SH-SAW (ex: Love waves) or “shear-vertical” SV-SAW (Rayleigh waves). Rayleigh waves involve a deformation of the substrate in the direction normal to the surface. When an alternating voltage is applied to the IDT electrodes at the resonant frequency (which depends on the nature of the material, cut, and wave propagation direction),

*Biophotonics and Optoelectronics laboratory, Université de Sherbrooke, Sherbrooke, Québec, Canada. E-mail: Paul.Charette@USherbrooke.ca; Fax: +1 (819) 821-7937; Tel: +1 (819) 821-8000 x63861*

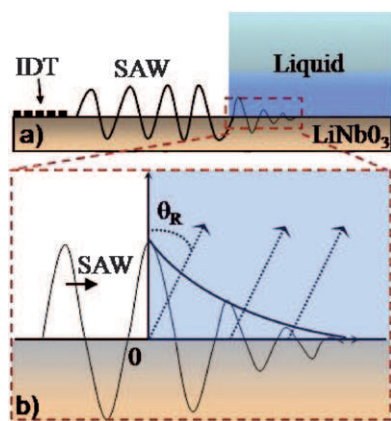


**Fig. 1** (a) Schematic diagram showing interdigitated transducer (IDT) metal electrodes on a LiNbO<sub>3</sub> piezoelectric substrate and the propagation along the surface of shear-vertical SAW (SV-SAW). (b) Zoomed view showing the acoustic energy radiated into the fluid at the Rayleigh angle,  $\theta_R$ , leading to acoustic streaming in the fluid.

SAW are generated and propagate along the surface.<sup>8</sup> It is well known that SV-SAW provide accelerated microfluidic mixing at the liquid-solid interface.<sup>9</sup> SV-SAW transmit mechanical energy into the fluid at the Rayleigh angle,  $\theta_R$ , as shown in Fig. 1, both by mechanical deformation of the surface and *via* the electric field, inducing turbulent flow within the fluid.

This phenomenon, known as acoustic streaming,<sup>10</sup> can generate very large velocity gradients in fluids and has been shown to accelerate the process of analyte capture on a biosensing surface through agitation of the fluid containing the target analytes.<sup>11</sup> In addition, stronger SAW mechanical perturbations have been shown to remove nonspecifically adsorbed molecules from the sensing surface without disrupting subsequent biological activity.<sup>12,13</sup>

### Surface plasmon resonance (SPR)

SPR is a phenomenon whereby light couples to surface plasmons at the interface between two materials having permittivities of opposite sign, typically a metal and a dielectric.<sup>2</sup> The energy coupling efficiency between the excitation light and surface plasmons is sensitive to minute changes in the nature (chemical species, thickness, temperature, *etc.*) of the molecular layer in close proximity (within  $\sim 200$  nm for visible light) to the metal surface (the sensing area). Such changes manifest themselves as a variation in reflectivity at a given excitation/reflection angle, or as a shift in the angular position of the reflectivity minimum (maximum coupling). A significant advantage of SPR over other detection techniques is that it does not require labelling of target analytes, in contrast to fluorescence or radioactive isotope methods.

### Prior work combining SAW and SPR

Galopin *et al.*<sup>14</sup> described combining SPR and SV-SAW for biosensing, but as two separate devices situated on opposite inner surfaces of a microfluidic channel. Although this configuration is appropriate for SAW-accelerated mixing in a thin enough channel, it cannot benefit from the increased sensitivity afforded

by the active desorption of nonspecifically-bound parasitic biomolecules because the SAW are not generated on the sensing surface. In addition, their design is not suited to systems requiring an open configuration without flow such as microfluidic wells.

Francis *et al.*<sup>15</sup> demonstrated a common-substrate bimodal sensor system where SAW are used for sensing viscoelastic properties of materials in complement to standard SPR molecular binding measurements. Though the SPR and SAW transducers are on the same substrate, the SAW are used for sensing, not for mixing. Indeed, the type of SAW used in this case are shear-horizontal SH-SAW (Love wave) which oscillate in the plane of the surface without coupling acoustic energy into the liquid, and hence have no microstreaming effect.<sup>16</sup>

## SV-SAW and SPR integrated on a common substrate

### Design and fabrication

The objective of this work was to combine SPR and Rayleigh-type SV-SAW transducers on a common piezoelectric substrate. We took advantage of the fact that the fabrication of both the SAW and SPR devices involves the deposition of thin metal films on the top side of the substrate, leaving the back side available for light injection in a classic prism-based Kretschmann SPR configuration (Fig. 2).

Integrated SPR/SAW chips were fabricated on an X-cut LiNbO<sub>3</sub> substrate. LiNbO<sub>3</sub> (optical birefringence:  $n_e = 2.2$  and  $n_o = 2.287$  at 633 nm)<sup>17</sup> was chosen for its excellent optical properties in the visible and near-IR ranges and its good electromechanical coupling coefficients,  $K$ , along both Y and Z perpendicular propagation directions ( $K_x^2 = 5.9\%$ ,  $K_y^2 = 3.1\%$ ). Indeed, the  $K^2$  values along the two directions are more balanced than for a typical 128° Y-X cut crystal ( $K_x^2 = 5.6\%$ ,  $K_y^2 = 1.2\%$ ). The acoustic wavelength,  $\lambda_a$ , is equal to the pitch or “finger period”,  $2d$  (Fig. 2). The operating frequency,  $f_0$ , is related to the mechanical wave propagation speed in the substrate,  $v$ , by:

$$f_0 = v/2d$$

where  $f_0 = 20$  MHz and  $\lambda_a = 2d = 180$   $\mu\text{m}$  in the design shown in Fig. 2. The SAW transducer electrodes consist of 10 double split-finger pairs per IDT. An excitation voltage of frequency  $f_0$  applied to the transducer generates the acoustic waves.

In terms of manufacturability, both the SPR sensor and IDT electrodes involve low-resolution microfabrication processes (metal deposition by evaporation followed by lift-off in our case) so that they can be fabricated simultaneously on the common substrate. Typical metals used include silver, copper, and aluminium, with gold being the most common. To avoid mechanical loading of the surface which would disperse the SAW, electrode thickness must be much less than  $\lambda_a$ . In our work, the IDT electrodes and SPR sensing surface were fabricated using 48 nm-thick Au films atop a 3nm-thick Cr adhesion layer.

Note finally that, as in the case of our initial experiments, when the excitation light source is coherent (*i.e.* from a laser) and the substrate has “optically flat” surfaces, the substrate top and bottom surfaces must be slightly bevelled with respect to each other in order to eliminate self-interference artefacts caused by

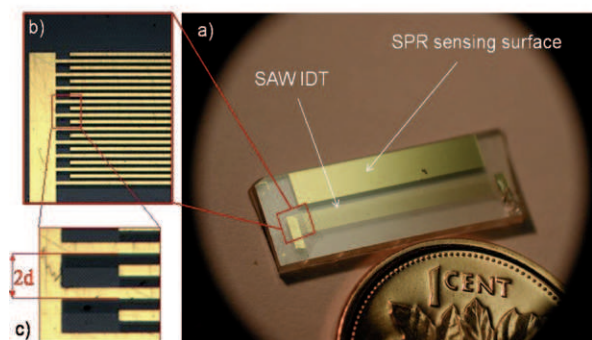
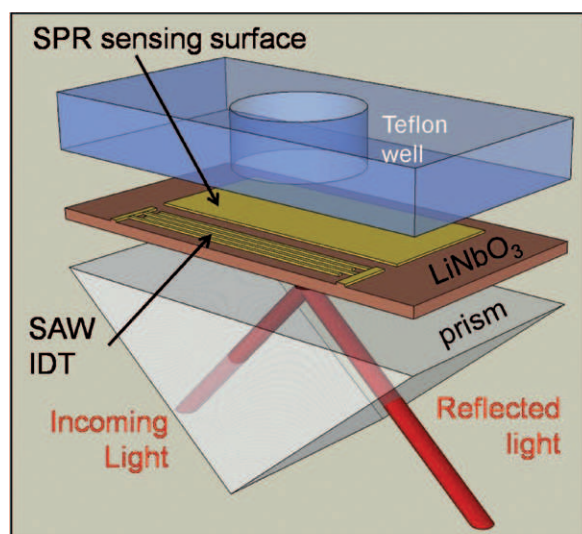


**Fig. 2** TOP: Schematic diagram of the integrated device showing the SPR sensing surface and SAW IDT electrodes on a common LiNbO<sub>3</sub> piezoelectric substrate. Also shown are the SPR excitation and reflected light paths that are coupled to the sensing surface *via* the prism, as well as the microfluidic well atop the SPR sensing surface. BOTTOM: (a) top view of the IDT electrodes and SPR sensing surface (48 nm thickness Au film with a 3 nm thickness Cr adhesion layer) on the LiNbO<sub>3</sub> substrate; (b) and (c): zoomed views of the IDT electrodes ( $2d = 180 \mu\text{m}$ ).

multiple reflections. Beveling is not required with glass substrates typically used for SPR because the glass surfaces are not optically flat.

## Experimental results

### Methods

Experiments were performed at room temperature on a custom-built SPR apparatus described in detail in a previous publication.<sup>18</sup> SPR/SAW chips are placed on top of a SF10 glass ( $n = 1.723$ ) coupling prism with index matching fluid ( $n = 1.735$ ). Collimated light from a linearly-polarized 4 mW stabilized laser diode (635 nm) passes through the prism and is reflected off the back-surface of the metal film, passes through a motorized linear polarizer, and is incident onto a detector. The laser diode is oriented about its optical axis such that equal amounts of energy are injected into the s- and p-polarizations. As only the p-polarization can be coupled to surface plasmons, the s-polarization is used as a reference to remove the dependence on laser

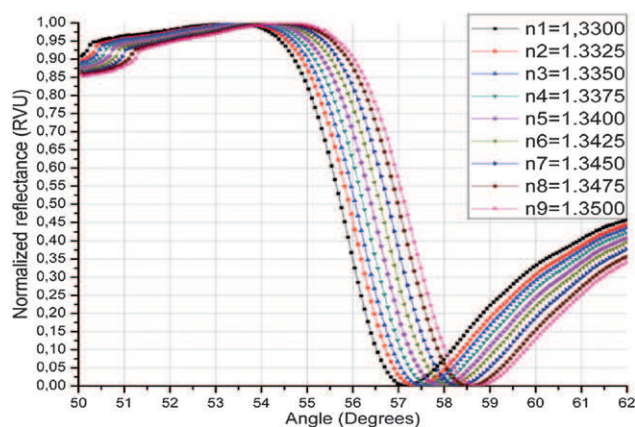


**Fig. 3** Experimental results obtained with the integrated SPR/SAW chip showing the SPR reflectivity curves as a function of incidence angle for 9 liquids with calibrated optical refractive indices ( $n_1 = 1.3300$ ,  $n_2 = 1.3325$ ,  $n_3 = 1.3350$ ,  $n_4 = 1.3375$ ,  $n_5 = 1.3400$ ,  $n_6 = 1.3425$ ;  $n_7 = 1.3450$ ,  $n_8 = 1.3475$  and  $n_9 = 1.3500$ ). Results are given in reflectance variation units (RVU), where 1 RVU equals 100% reflectance change.

power drift and other time-dependant noise sources, as well as for normalization. The fluidic well (200  $\mu\text{l}$ ) is clamped on top of the SPR/SAW chip. Reflectance as a function of angle is measured by mechanically scanning the laser and detector at equal and opposite angles.

### SPR on a piezoelectric substrate (LiNbO<sub>3</sub>)

Fig. 3 shows (raw, unfiltered) results from a first validation experiment where reflectance is plotted against light incidence angle for a set of fluids having calibrated refractive indices ranging from 1.3300 to 1.3500 (Cargille Labs, USA). As expected, the results show SPR reflectivity curves shifting to the right (larger angles of minimum reflectivity) with increasing refractive index. This experiment demonstrates that SPR can be performed on a LiNbO<sub>3</sub> substrate with results very similar to that obtained with glass substrates, a prerequisite for combining SAW and SPR on a common piezoelectric substrate.

### SPR and SAW: temperature effects

SPR sensors respond to changes in refractive index in the dielectric medium above the metal film within the usable range of the evanescent field. Hence, any process that affects the refractive index in close proximity to the metal surface, whether it be due to changes in the chemical nature of the dielectric or its properties (such as temperature), can potentially generate an SPR signal. In the case of an aqueous medium, the dependence between temperature and refractive index changes is in the order of  $1 : 10^{-4}$  around room temperature.<sup>19</sup> Therefore, a 0.1 °C temperature change in the liquid medium will cause a  $10^{-5}$  refractive index unit (RIU) change in the medium, a measurable signal in sensitive SPR systems that may be misinterpreted as a change in surface chemistry (binding or release of ligands).

Such temperature-related noise is a particularly important issue when combining SPR with SAW. Indeed, as a direct consequence of the mechanical and electrical energy coupling between SV-SAW and a fluid, heat is injected into the fluid thereby causing

localized temperature changes. SAW have in fact been used to control temperature in fluids.<sup>20</sup> Fortunately, compared to the thin film of fluid above the surface that is directly perturbed by the SAW, the majority of the fluid volume in the microfluidic system (well or channel) is outside the SAW-fluid heat coupling range and should act as a heat sink. We therefore postulated that temperature increases in the fluid at the metal surface due to a SAW pulse would dissipate after a suitable relaxation time. We conducted a series of experiments to study SPR measurement noise caused by SAW action to validate this hypothesis.

In the experiments, SAW excitation characteristics (pulse period, duty cycle, power, relaxation time) appropriate for inducing microstreaming in the fluid (water) were varied independently while monitoring SPR reflectance variations. Experiments were conducted using an RF signal generator (N5181A, 250 kHz to 1 GHz bandwidth, Agilent, USA) and custom-built power amplifier (30 dBm gain, 25 W maximal unsaturated output power, 0.15 MHz–230 MHz bandwidth, Empower RF Systems, USA), controlled by a custom LabView application.

Fig. 4 shows changes in SPR reflectance at a fixed angle of interrogation for several SAW electrical excitation power levels ( $P_1 = 37$  dBm to  $P_{10} = 28$  dBm). Results are given in reflectance variation units (RVU), where 1 RVU represents 100% variation in reflectance. For each case, the SAW excitation was applied for 5 s and then stopped. Following each application of SAW, the time required for the liquid medium to return to its equilibrium temperature (relaxation time) was determined by measuring the time taken for the SPR signal to return to a stable plateau. Within measurement error, the relaxation times ranged from 300 s to 30 s, with a roughly linear dependence of relaxation time on power level in dBm, over the range of power levels tested.

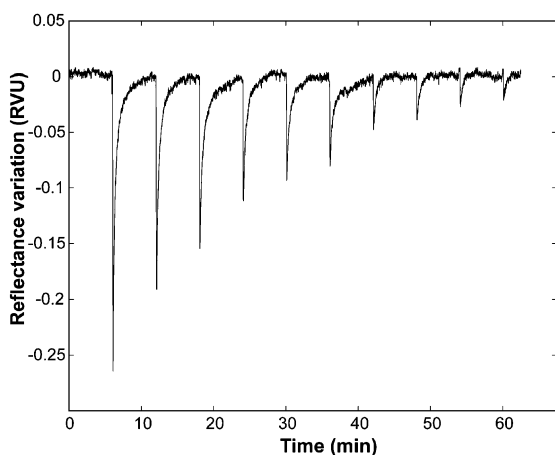


**Fig. 4** Plot of SPR reflectance variation over time at a fixed interrogation angle, showing the effect on the SPR response of heat injection into the fluid (water) caused by single SAW pulses of various power levels. For each power level (37 dBm to 28 dBm, in increments of 1 dBm), the SAW were excited for 5 s then turned off to allow the system to return to a stable plateau before the next SAW pulse. Results are given in reflectance variation units (RVU), where 1 RVU equals 100% reflectance change.

#### SAW-induced microfluidic mixing with an avidin-biotin assay

Fig. 5 illustrates the performance of the SPR/SAW chip for measuring assay binding kinetics. SPR reflectance variations are

shown as a function of time at a fixed angle of interrogation for a standard assay: biotin-avidin in phosphate buffer solution (PBS, Wisent, Canada). Biotinylated bovine serum albumin (BSA-biotin, 0.1 mg ml<sup>-1</sup>, Sigma-Aldrich, USA) was first introduced into the fluidic well using a micropipette and allowed to adsorb onto the gold surface. Once the reaction had reached equilibrium (SPR signal plateau), the well was rinsed with buffer solution and emptied using aspiration six times. Avidin (5 μg ml<sup>-1</sup>, Sigma-Aldrich, USA) was then introduced into the fluidic well using a micropipette.

Experiments were performed at room temperature under identical conditions, save for SAW power levels. Starting at the time of avidin introduction (time = 0 in the graphs), SAW excitation was applied in 5 s-duration pulses followed by 120 s

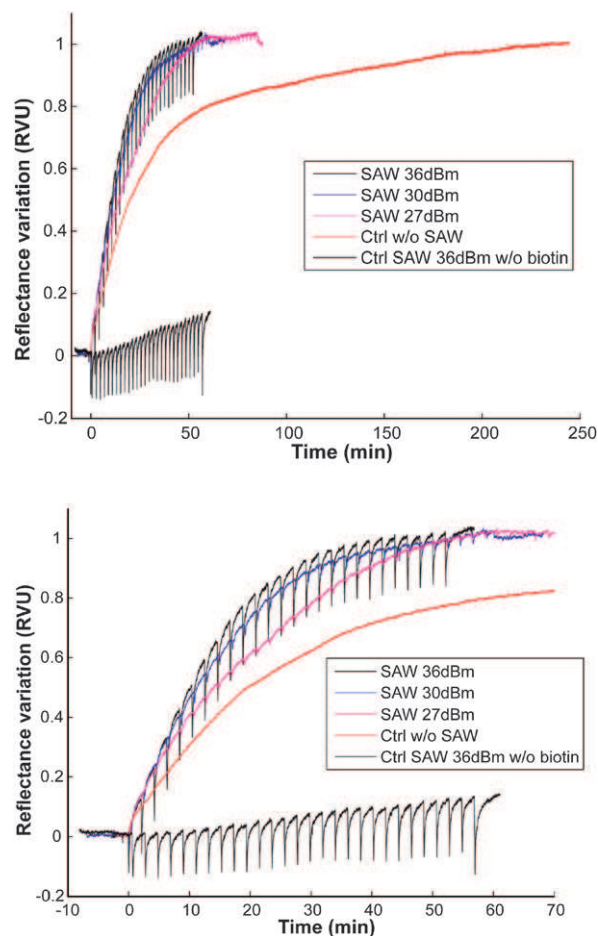


**Fig. 5** Graphs showing SPR reflectance variations at a fixed angle of interrogation as a function of time, for a biotin-avidin assay in PBS (avidin is introduced at time = 0). Periodic SAW excitation was applied in 5 s-duration pulses followed by 120 s relaxation intervals, for a range of SAW power levels (27, 30, 36 dBm). A negative control without the application of SAW in the avidin-biotin assay is shown (Ctrl w/o SAW). A negative control where unbiotinylated BSA was adsorbed onto the surface followed by injection of avidin under 36dBm SAW is also shown (Ctrl SAW 36dBm w/o biotin). TOP: full time scale; BOTTOM: Zoomed view. The downward spikes clearly visible in the 36dBm data are due to heat injection into the fluid by the SAW pulses (the effect of heat injection at lower SAW power is barely visible). Results are given in reflectance variation units (RVU), where 1 RVU equals 100% reflectance change.

relaxation intervals, for a range of SAW power levels (27, 30, 36 dBm). Data were normalized with respect to their respective equilibrium plateaus, which differed very slightly between experiments due to normal variations in the substrate fabrication process. A negative control (BSA-biotin/avidin assay) without the application of SAW is also shown in Fig. 5. These experiments show that SAW action results in greatly accelerated kinetics compared to the negative control, due to microfluidic mixing ( $\sim 5\times$  compared to the negative control for these particular experiments).

Note also that since temperature increases in the fluid due to heating by the SAW pulses result in a decrease in reflectance whereas avidin binding results in an increase in reflectance, the binding curve envelope cannot be attributed to thermal effects. Indeed, the results demonstrate that the chip recovers well from the heat injection pulses (downward spikes in the data) with the binding curve maintaining an exponential envelope, as expected for this type of assay.

Experiments performed with higher SAW power levels resulted in curves with an envelope that was identical to that of the 36 dBm curve, indicating that the chip had achieved a maximum mixing efficiency for that particular SAW/SPR design. Power levels of 30 and 27 dBm also resulted in accelerated kinetics but with intermediate levels of mixing efficiency. Finally, Fig. 5 shows a second negative control experiment where SAW were applied at 36 dBm, but where unbiotinylated BSA was adsorbed onto the surface, followed by injection of avidin.

## Conclusions

We have presented an integrated chip incorporating SPR sensing and SAW microfluidic mixing on a common substrate. Validation experiments show that, with appropriate electrical excitation parameters, SAW-induced mixing results in greatly accelerated binding kinetics. Results also show that, though SAW action causes an unwanted parasitic SPR response due to heat injection into the fluid, a relatively brief relaxation time following SAW pulses will allow this effect to dissipate without affecting the overall assay response. These findings should lead to more timely and sensitive assays in SPR-based biosensors and lab-on-chip devices. Since both SPR sensors and SAW transducers can be fabricated simultaneously on a single substrate using low-cost microfabrication methods, the proposed design is well-suited to lab-on-chip applications.

Note finally that optimal SAW operating conditions are unique to a particular set of experimental conditions and chip design. Indeed, depending on the assay involved, SAW-induced microfluidic mixing and desorption may be required to be more or less vigorous. Therefore, the experimental results presented here are not meant to be exhaustive or to identify a globally optimal set of SAW excitation parameters, but rather to illustrate the operational parameters that must be tuned through typical examples. Operating conditions must therefore be optimized on a case-by-case basis.

## Acknowledgements

This work was supported in part by grants from the Natural Sciences and Engineering Research Council of Canada

(NSERC). The authors wish to thank the staff of the CRN<sup>2</sup> (Centre de recherche en nanofabrication et nanocaractérisation) at the Université de Sherbrooke for their help and advice.

## Notes and references

- 1 R. L. Rich and D. G. Myszka, Survey of the year 2007 commercial optical biosensor literature, *J. Mol. Recognit.*, 2008, **21**(6), 355–400.
- 2 J. Homola, Surface plasmon resonance sensors for detection of chemical and biological species, *Chem. Rev.*, 2008, **108**(2), 462–493.
- 3 N. Miura, D. R. Shankaran and K. V. Gobi, Recent advancements in surface plasmon resonance immunosensors for detection of small molecules of biomedical, food and environmental interest, *Sens. Actuators, B*, 2007, **121**(1), 158–77.
- 4 E. Ostuni, R. G. Chapman, R. E. Holmlin, S. Takayama and G. M. Whitesides, A survey of structure-property relationships of surfaces that resist the adsorption of protein, *Langmuir*, 2001, **17**(18), 5605–5620.
- 5 T. M. Squires, R. J. Messinger and S. R. Manalis, Making it stick: convection, reaction and diffusion in surface-based biosensors, *Nat. Biotechnol.*, 2008, **26**(4), 417–426.
- 6 A. Renaudin, P. Tabourier, J.-C. Camart and C. Druon, Surface acoustic wave two-dimensional transport and location of microdroplets using echo signal, *J. Appl. Phys.*, 2006, **100**(11), 116101–1.
- 7 D. S. Lee Y. Q. Fu S. Maeng X. Y. Du S. C. Tan, J. K. Luo, A. J. Flewitt, S. H. Kim, N. M. Park, Y. J. Choi, H. C. Yoon, S. Y. Oh and W. I. Milne., Integrated ZnO surface acoustic wave microfluidic and biosensor system, in *IEEE International Electron Devices Meeting - IEDM '07*, Washington, DC, USA, 2007.
- 8 A. Renaudin, P. Tabourier, V. Zhang, J. C. Camart and C. Druon, SAW nanopump for handling droplets in view of biological applications, *Sens. Actuators, B*, 2006, **113**(1), 389–397.
- 9 K. Sritharan, C. J. Strobl, M. F. Schneider, A. Wixforth and Z. Guttenberg, Acoustic mixing at low Reynold's numbers, *Appl. Phys. Lett.*, 2006, **88**(5), 054102.
- 10 T. Wei-Kuo, L. Jr-Lung, S. Wang-Chou, C. Shu-Hui and L. Gwo-Bin, Active micro-mixers using surface acoustic waves on Y-cut 128° LiNbO<sub>3</sub>, *J. Micromech. Microeng.*, 2006, **16**(3), 539–48.
- 11 L. A. Kuznetsova and W. T. Coakley, Applications of ultrasound streaming and radiation force in biosensors, *Biosens. Bioelectron.*, 2007, **22**(8), 1567–1577.
- 12 S. Cular, D. W. Branch, V. R. Bhethanabotla, G. D. Meyer and H. G. Craighead, Removal of Nonspecifically Bound Proteins on Microarrays Using Surface Acoustic Waves., *IEEE Sens. J.*, 2008, **8**(3), 314–320.
- 13 G. D. Meyer, J. M. Morán-Mirabal, D. W. Branch and H. G. Craighead, Nonspecific Binding Removal From Protein Microarrays Using Thickness Shear Mode Resonators, *IEEE Sens. J.*, 2006, **6**(2), 254–261.
- 14 E. Galopin, M. Beaugeois, B. Pinchemel, J. C. Camart, M. Bouazaoui and V. Thomy, SPR biosensing coupled to a digital microfluidic microstreaming system, *Biosens. Bioelectron.*, 2007, **23**(5), 746–50.
- 15 J. M. Friedt, L. Francis, G. Reekmans, R. De Palma, A. Campitelli and U. B. Sleytr, Simultaneous surface acoustic wave and surface plasmon resonance measurements: electrodeposition and biological interactions monitoring, *J. Appl. Phys.*, 2004, **95**(4), 1677–80.
- 16 C. Zhang, J. J. Caron, and J. F. Vetelino. The Bleustein-Gulyaev wave mode in potassium niobate for liquid sensing applications, in *IEEE Ultrasonics Symposium*, San Juan, 2000.
- 17 U. Schlarb and K. Betzler, Refractive indices of lithium niobate as a function of wavelength and composition, *J. Appl. Phys.*, 1993, **73**(7), 3472–3476.
- 18 V. Chabot, C. M. Cuerrier, E. Escher, V. Aimez, M. Grandbois and Paul G. Charette, Biosensing based on surface plasmon resonance and living cells, *Biosens. Bioelectron.*, 2009, **24**(6), 1667–1673.
- 19 J. H. Grassi and R. M. Georgiadis, Temperature-Dependent Refractive Index Determination from Critical Angle Measurements: Implications for Quantitative SPR Sensing, *Anal. Chem.*, 1999, **71**(19), 4392–4396.
- 20 J. Kondoh, N. Shimizu, Y. Matsui, M. Sugimoto and S. Shiokawa, Development of temperature-control system for liquid droplet using surface Acoustic wave devices, *Sens. Actuators, A*, 2009, **149**(2), 292–297.